Minidisk Dynamics in Accreting, Spinning Black Hole Binaries: Simulations in Full General Relativity

Vasileios Paschalidis[1,2] , Jane Bright[1], Milton Ruiz[3] , and Roman Gold[4]
[1] Department of Astronomy, University of Arizona, Tucson, AZ 85726, USA
[2] Department of Physics, University of Arizona, Tucson, AZ 85726, USA
[3] Department of Physics, University of Illinois at Urbana-Champaign, Urbana, IL 61801, USA
[4] CP3 origins|Southern Denmark University (SDU) Campusvej 55, Odense, Denmark

Abstract

We perform magnetohydrodynamic simulations of accreting, equal-mass binary black holes in full general relativity focusing on the impact of black hole spin on the dynamical formation and evolution of minidisks. We find that during the late inspiral the sizes of minidisks are primarily determined by the interplay between the tidal field and the effective innermost stable orbit around each black hole. Our calculations support that a minidisk forms when the Hill sphere around each black hole is significantly larger than the black hole's effective innermost stable orbit. As the binary inspirals, the radius of the Hill sphere decreases, and minidisks consequently shrink in size. As a result, electromagnetic signatures associated with minidisks may be expected to gradually disappear prior to merger when there are no more stable orbits within the Hill sphere. In particular, a gradual disappearance of a hard electromagnetic component in the spectrum of such systems could provide a characteristic signature of merging black hole binaries. For a binary of given total mass, the timescale to minidisk "evaporation" should therefore depend on the black hole spins and the mass ratio. We also demonstrate that accreting binary black holes with spin have a higher efficiency for converting accretion power to jet luminosity. These results could provide new ways to estimate black hole spins in the future.

1. Introduction

Supermassive black hole (SMBH) binaries are expected to form in gas rich environments as a result of galaxy mergers (Rodriguez et al. 2009). These systems form unique sources for multimessenger signals. SMBH binary evolution is particularly promising as potentially strong sources of gravitational and various forms of electromagnetic emission. Gravitational waves from SMBH binaries are expected to be detectable by Pulsar Timing Arrays or by future space-based gravitational wave observatories such as the Laser Interferometer Space Antenna (LISA; Hobbs et al. 2010; Amaro-Seoane et al. 2017). Recently, observational efforts searching for such systems have yielded an unprecedented number of exciting candidate sources based on various diagnostics including periodicities in light curves, spectral features such as double-horned emission lines, and (lensing) flares (see, e.g., Drake et al. 2009; Graham et al. 2015; Charisi et al. 2016; Hu et al. 2020). A main challenge in these efforts is our lack of understanding of the unique features the electromagnetic emission from these systems has. As a result, much of the theoretical work on accreting binary black holes to-date has focused on identifying interesting characteristic electromagnetic signatures that accompany their gravitational wave signals.

In this paper we investigate the conditions under which minidisks form around each individual black hole in the late stages of the binary black hole inspiral. It has been argued that minidisks are responsible for the emission of the hardest part of the electromagnetic spectrum due to shock heating (Sesana et al. 2012; Roedig et al. 2014; Farris et al. 2015). Emission from the hot minidisks could make up for any "notch" in the high frequency spectrum that might be expected due to the lack

of gas in the disk cavity during the inspiral phase. Minidisks could also be responsible for providing modifications to broad emission-line profiles (Nguyen et al. 2019). The potentially observable electromagnetic (EM) emission originating from minidisks (d'Ascoli et al. 2018) as well as the possibility to use them as "smoking-gun" features to identify SMBH binaries, makes understanding the conditions under which minidisks form and maintain a persistent structure toward the late stages of the inspiral a vital goal. Minidisks have been seen in some recent Newtonian studies, e.g., Farris et al. (2014, 2015), and studies with approximate spacetime metrics (Bowen et al. 2017, 2018), but not in previous studies in full general relativity, e.g., Farris et al. (2012); Gold et al. (2014a, 2014b), highlighting the need to investigate the conditions for minidisk formation in relativistic gravitation. The studies using approximate spacetime metrics focusing on near equal-mass systems (Bowen et al. 2017, 2018, 2019), initialize the simulations with minidisks in addition to the circumbinary disk, but do not report persistent, steady-state minidisks. Instead, those works report cycles of depletion and replenishment as well as sloshing of mass between the two minidisks.

Previous theoretical work on circumbinary disks incorporating varying degrees of relativistic gravity and magnetic fields include Farris et al. (2012, 2014), Giacomazzo et al. (2012), Noble et al. (2012), Gold et al. (2014a, 2014b), Kelly et al. (2017), Bowen et al. (2018), Khan et al. (2018), Bowen et al. (2019), and Armengol et al. (2021), but only a subset of these focus on circumbinary accretion, see Gold (2019) for a recent review. Gold et al. (2014b) proposed that circumbinary disks form minidisks whenever there are stable circular orbits within the Hill sphere around each black hole. In this work we perform simulations in full general relativity (GR) to test this

hypothesis. Our approach makes no approximation for the spacetime metric and as a result we do not have to excise parts of the domain and/or impose ad hoc inflow boundary conditions. Instead, the black holes are resolved objects on our computational grid. The duration of our simulations are significantly shorter than in some earlier treatments. However, the regime of minidisks that is probed here exhibits much shorter relaxation times.

The analysis we follow is guided in part by the restricted three-body Newtonian problem, where one can define regions in which gravity is dominated by each of the binary components, as quantified by the Hill sphere $r_{Hill} = 0.5(q/3)^{1/3}d$. Here q is the mass ratio and d is the binary separation. While the systems studied here are not in the Newtonian regime, it is still expected that many Newtonian aspects carry over to the relativistic regime with some appropriate corrections. On the other hand, it is well-known that stable circular orbits (and hence disks) around general relativistic black holes can exist only outside the innermost stable circular orbit (ISCO) $r_{ISCO} = r_{ISCO}(\chi)$ where χ is the dimensionless black hole spin parameter satisfying $|\chi| \leqslant 1$. Therefore, the expectation is that minidisks can form early on in the inspiral at binary separations that satisfy $r_{Hill} \gg r_{ISCO}(\chi)$, so that stable orbits around each black hole can exist within the Hill sphere (Gold et al. 2014b). However, in the later stages of the inspiral when $r_{Hill} \sim r_{ISCO}(\chi)$ no stable orbits exist within the Hill sphere and matter is quickly accreted as soon as it enters the Hill sphere. For an equal-mass, nonspinning system, we can perform a simple Newtonian estimate which yields $r_{Hill} = 0.5(q/3)^{1/3}d \sim 0.35d$ and $r_{ISCO} = 3M$, setting these equal gives a threshold separation for minidisks to exist $d_{thres} \simeq 8.7M$. In particular, one would require $d \gg d_{thres}$ for persistent minidisks to exist. As the binary inspirals d approaches d_{thres}, and any persistent minidisks should evaporate.

Astrophysical black holes are expected to have spin (Lynden-Bell 1969). X-ray reflection measurement techniques have been used in over two dozen AGN systems to determine the spins of the SMBHs, and have found that the majority of these systems are rapidly rotating with $\chi \geqslant 0.9$, while the most massive SMBHs ($\gtrsim 10^8 M_\odot$) have slower, but still significant spins in the range of $\chi \sim 0.5$–0.7 (Reynolds 2019). As spin is crucial to determine the ISCO, incorporating spin into our study of minidisks is important both for astrophysical implications, e.g., jets, and for providing a clear diagnostic for testing our hypothesis regarding minidisk formation.

By performing magnetohydrodynamic simulations in full GR of $q = 1$ binary black holes with spins both (anti)aligned with the orbital angular momentum, and one aligned and the other antialigned we demonstrate explicitly the impact of spin in allowing the formation of minidisks, thereby confirming the expectations from Gold et al. (2014b) that minidisks should form only when stable orbits exist within the Hill sphere around each black hole. In addition, we demonstrate the importance of spin on jet outflows as we find that spinning binaries have stronger jet luminosities.

In the fully relativistic circumbinary accretion studies of Farris et al. (2012) and Gold et al. (2014a, 2014b) the launching of jets from the interaction of magnetic fields with black hole horizons, even for nonspinning binary black holes, had already highlighted the importance of full GR in

discovering features that are entirely missed in Newtonian studies, and studies that include varying degrees of relativity, but still do not capture black hole horizons. Minidisk evaporation as discussed in this work highlights yet another effect in which GR plays a key role in determining even the qualitative behavior.

The rest of the paper is structured as follows. In Section 2 we present the initial data, grids, and numerical methods we adopt for our evolutions. In Section 3 we present our results, and summarize in Section 4. We denote the total binary mass M and both the primary and secondary mass m. We set $G = c = 1$.

2. Methods and Initial Data

In this work we evolve the spacetime metric by solving Einstein's field equations in the BSSN formulation (Shibata & Nakamura 1995; Baumgarte & Shapiro 1999). Our methods for solving Einstein's field equations for the gravitational field, and the equations of ideal magnetohydrodynamics in curved spacetime have been described previously in Khan et al. (2018), where we refer the reader for more details and further references. Our code has been extensively tested against the majority of GR magnetohydrodynamics (GRMHD) codes in the context of single black hole spacetimes in Porth et al. (2019). As in Khan et al. (2018) we use puncture initial data for the spacetime metric adopting the TwoPunctures code (Ansorg et al. 2004), but set the black holes initially on a quasicircular orbit at a larger coordinate separation of 20M. We also treat black hole spin for the first time in full GR calculations of circumbinary accretion. We consider equal-mass binaries in four spin configurations: $\chi_1 = \chi_2 = 0$ (non-spinning case labeled χ_{00}), $\chi_1 = \chi_2 = 0.75$ (case χ_{++}), $\chi_1 = \chi_2 = -0.75$ (case χ_{--}), and $\chi_1 = -\chi_2 = 0.75$ (case χ_{+-}), where χ_1 and χ_2 are the dimensionless spins of each black hole, and the $+$ $(-)$ sign indicates spin aligned (antialigned) with the orbital angular momentum. The matter and magnetic field initial data are identical to those in Gold et al. (2014a) and the same for all binary configurations we study. The circumbinary disk and binary angular momenta are aligned. The equation of state corresponds to a $\Gamma = 4/3$ Γ-law, and there is no cooling employed during the evolution. We employ three sets of nested levels of mesh refinement: one centered on each black hole and one centered at the origin. The set centered on the origin has 10 levels of refinement, while those centered on the black holes have 12 levels for case χ_{00}, and 13 levels for cases with nonzero spin. We place the outer boundary at 3072M, and the resolution on the coarsest refinement level to 48M. The finest level resolution is $\simeq M/85$ ($\simeq M/43$) for cases with(without) spin. The black hole apparent horizon diameters are resolved by $\gtrsim 51$ ($\gtrsim 41$) grid points in their smallest dimension for the spinning (nonspinning) cases. The half-side lengths of the refinement boxes are given by $3072/2^n$, $n = 0, 1, \ldots 12$, where n indexes the levels of refinement with $n = 0$ denoting the coarsest level.

3. Results

Nonspinning black holes have an ISCO (areal) radius of $r_{ISCO} = 6m = 3M$. Prograde (retrograde) orbits around black holes with spin $\chi = 0.75$ have smaller (larger) $r_{ISCO} = 3.16m = 1.58M$ ($r_{ISCO} = 8.28m = 4.14M$), thereby allowing more (less) space for stable orbits within the black hole Hill sphere, making it easier (more difficult) for minidisks

to form. We use these radii as coordinate radii in our figures to indicate the location of the ISCO around each black hole. We point out that this is neither a gauge invariant, nor a precise measure for relativistic binaries. We only use these radii as an approximate way to visualize the ISCO in our figures.

We use the rest-mass density profiles, the mass contained within the Hill sphere of each black hole, and the accretion rates onto the black holes (as defined in Farris et al. 2010) as diagnostics for studying minidisk formation and evolution. The Hill sphere radius is computed based on the Newtonian formula $r_{\mathrm{Hill}} = 0.5(q/3)^{1/3}d$, within which we integrate the total rest mass. This definition of the Hill sphere is based on the coordinate radius, it is not gauge invariant and is used only as a means to approximate the mass contained in minidisks. However, since the binary is symmetric this coordinate radius defines a volume around each black hole that is the same, which roughly coincides with the outer edges of the minidisks that form in our simulations as we show below. We also investigate the temperatures of the minidisks as well as the efficiency of converting accretion power to luminosity in each of our models.

The initial data were designed to probe the interplay of tidal forces and black hole spins to determine their impact on minidisks. In our earlier work, we did not find evidence for persistent minidisks. Minidisks would form and quickly be depleted. In those works the black holes were nonspinning ($r_{\mathrm{ISCO}} = 6m = 3M$) and the initial separation was $d = 10M$, and hence a Hill sphere of $r_{\mathrm{Hill}} \sim 3.5M$, leaving almost no room for stable orbits within the Hill sphere. By contrast, in this study, the initial separation is $d \sim 20M$, providing a larger Hill sphere of $r_{\mathrm{Hill}} \simeq 7M$, which leaves plenty of room for stable orbits for $\chi = 0.75$ black holes, some room in the $\chi = 0$ black holes, and little room in the $\chi = -0.75$ black holes. Therefore, the expectation is that persistent minidisks should more easily form dynamically around $\chi = 0.75$ black holes, but not so much around $\chi = -0.75$ black holes. This is consistent with our findings as we next discuss.

3.1. Rest-mass Density

As in our previous studies the matter undergoes a transient phase as the initial data is relaxed, and the accretion-flow regions closer to the black holes begin to settle after a time period $\Delta t \simeq 2000M$, as determined by the saturation of the mass accretion rate onto the black holes $\dot{M}$. This is consistent with typical findings in single black hole accretion studies (see Porth et al. 2019 and references therein), where it takes a few local orbital periods for turbulence to fully develop. The accretion flow settles in an inside-out fashion. Secular trends from an incomplete relaxation at larger radii should be present, but we do not expect this to affect our main conclusions. Minidisk structures form even before the accretion rate saturates and then settle down to a quasi-steady state around the same time.

In Figure 1 we show equatorial rest-mass density snapshots from case χ_{+-}. This case is the most unambiguous demonstration of the effect of spin on minidisk formation. For the $\chi = +0.75$ black hole r_{Hill} is significantly larger than r_{ISCO}, while for $\chi = -0.75$ black hole r_{ISCO} is comparable to r_{Hill}. As a result, we observe that the positive spin black hole develops a minidisk while the negative spin black hole does not. For the $\chi = -0.75$ black hole, material that enters the Hill sphere crosses the ISCO (solid white circles) shortly thereafter, and as a result the spiral streams are accreted without orbiting the black hole and forming a minidisk. We also observe that for all cases where persistent minidisks form, the outer edges of minidisks traces the approximate Hill sphere we draw (dashed black circles). This set of observations clearly demonstrates the validity of the argument that minidisks should form only when $r_{\mathrm{Hill}} \gg r_{\mathrm{ISCO}}$, resolving the question under what conditions minidisks can exist during the late stages of the inspiral.

In addition, we investigate our other models, χ_{00}, χ_{++}, and χ_{--}, to further support the findings of the χ_{+-} model. As expected from our earlier arguments, we find that cases χ_{00} and χ_{++} form persistent minidisks, while case χ_{--} ($r_{\mathrm{ISCO}} = 8.22m = 4.11M$) does not, and exhibits the same behavior as the $\chi = -0.75$ black hole in the χ_{+-} model, with spiral streams entering the Hill sphere and crossing the ISCO, and thereby plunging into the black hole. In Figure 2, we show an equatorial rest-mass density snapshot after five binary orbits have been completed for χ_{++}, and χ_{--}, demonstrating the above.

3.2. Rest-mass within Hill Spheres and Accretion Rates

We next investigate the rest mass contained within the Hill sphere of each black hole. The top left panel of Figure 3 shows the rest mass within the individual Hill spheres for the χ_{+-} case normalized to the time-averaged value of the total rest-mass within the Hill spheres of the χ_{00} case. The $\chi = +0.75$ black hole clearly contains more rest mass than the $\chi = -0.75$ one, demonstrating in another way that the matter plunges into the $\chi = -0.75$ black hole as soon as it enters the Hill sphere because it crosses the ISCO. A similar picture is painted by the top right panel in the same figure, which shows the total rest mass within the Hill spheres normalized to the time-averaged value of the total rest-mass within the Hill spheres of the χ_{00} case for cases χ_{00}, χ_{++}, and χ_{-}. As is clear from the image the total mass within the Hill spheres in the χ_{++} is about twice that of the χ_{00} model, which is about twice that of the χ_{-} model. However, the plots also demonstrate that the amount of rest-mass within the Hill sphere of even the $\chi = +0.75$ black holes, which form persistent minidisks, oscillates around a mean value in agreement with the nonspinning simulations reported in Bowen et al. (2017).

In the bottom left panel of Figure 3 we show the rest-mass accretion rate onto each black hole of the χ_{+-} model normalized by the time-averaged total accretion rate of the χ_{00} case. The plot clearly shows that the $\chi = -0.75$ black hole has a higher accretion rate than the $\chi = +0.75$ black hole, demonstrating the plunging of the accretion streams onto $\chi < 0$ black holes, as opposed to orbiting and forming minidisks around $\chi > 0$ black holes. In the bottom right panel we show the total rest-mass accretion rate normalized by the time-averaged total accretion rate of the χ_{00} case for cases χ_{00}, χ_{++}, and χ_{--}, with the horizontal lines indicating the time-averaged accretion rate for each case. As expected the time-averaged rest-mass accretion rate in the χ_{--} is larger than that in the χ_{00} case, which in turn is larger than in the χ_{++} case. The χ_{00}, χ_{++}, and χ_{--} cases reinforce our findings from the χ_{+-} model. The accretion rates exhibit clear periodicities, which will be the focus of a future paper of ours.

All these findings are consistent with the expectation that the location of the ISCO has a significant impact on the systems ability to maintain mass within the Hill spheres and form minidisks toward the late stages of the inspiral.
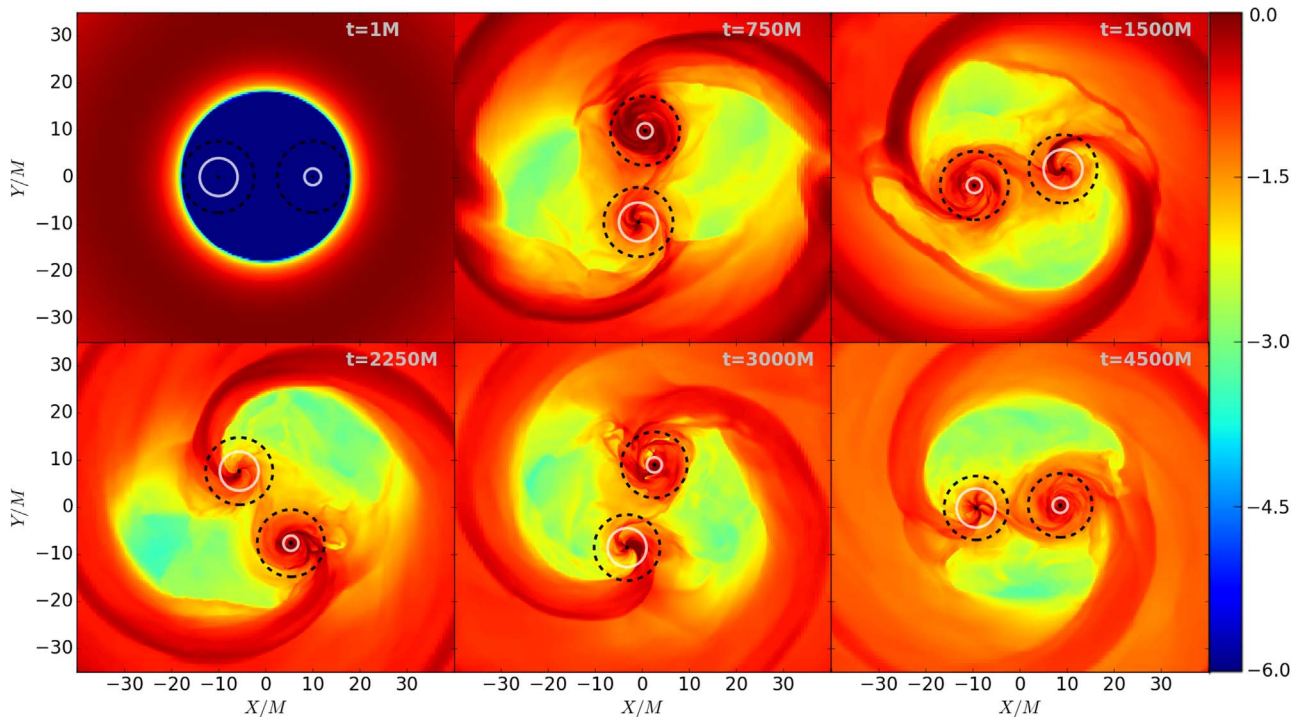
Figure 1. Rest-mass density in the equatorial plane for the χ_{+-} model. A persistent minidisk quickly forms around the $\chi_1 = +0.75$ black hole, but no disk forms around the $\chi_2 = -0.75$ black hole. The Hill spheres (black dashed circles) and the ISCO radii (white circles) are shown around each black hole (assuming each BH was in isolation). For the $\chi_1 = +0.75$ black hole the Hill sphere is significantly larger than the ISCO, but for the $\chi_1 = -0.75$ they are more comparable in size.
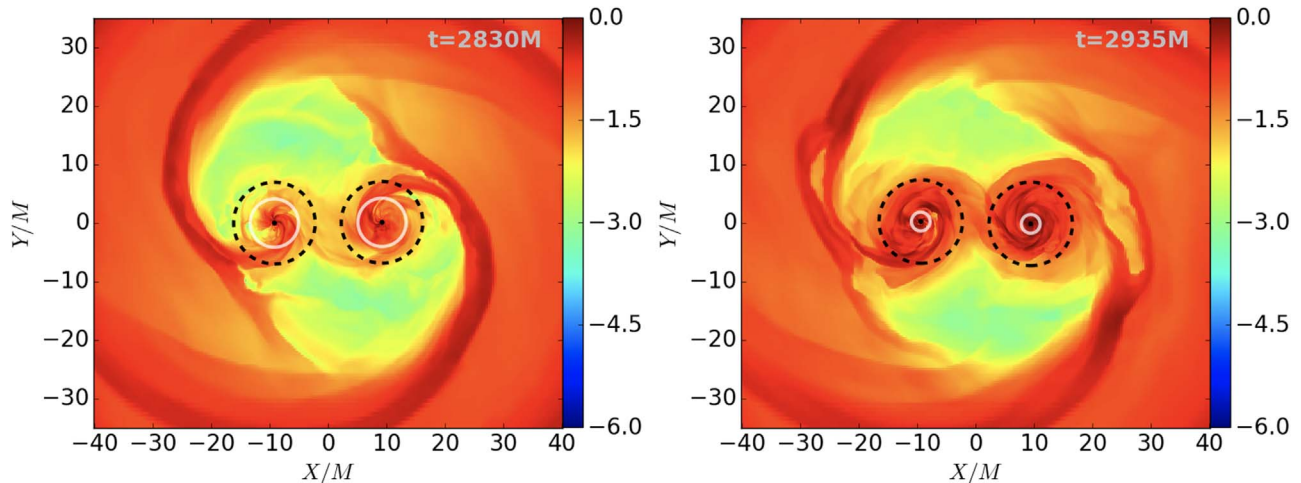
Figure 2. Comparison of the rest-mass density in the equatorial plane for χ_- (left panel) and χ_{++} (right panel), taken following completion of five orbits in both cases. Persistent minidisks are seen only in the χ_{++} case as the Hill sphere (black dashed circles) is significantly larger than ISCO radius (white circles).

3.3. Jet Luminosities and Temperatures

We find that jets are launched from both spinning and nonspinning systems as illustrated in Figure 4, which shows a 3D rendering of the rest-mass density of the χ_{++} model with white lines indicating the magnetic field lines anchored to the black holes. The magnetic field lines are more twisted than in the nonspinning cases we reported in earlier work (Gold et al. 2014a, 2014b; Khan et al. 2018)—a result of black hole spin. This combined effect leads to a dual jet structure close to the black holes that merge to form a single jet structure at larger height.

We calculate the Poynting luminosity associated with the collimated jet outflow on the surface of coordinate spheres S as

$L_{\rm EM} = \oint_S T^r_{0,(\rm EM)} dS$, where $T^\nu_{\mu,(\rm EM)}$ is the EM stress-energy tensor. $L_{\rm EM}/\dot{M}_{\rm eq}$ is the efficiency for converting accretion power to EM jet luminosity, where $\dot{M}_{\rm eq}$ is the time-averaged accretion rate after the accretion rate has settled ($t \gtrsim 1500M$). We plot the efficiency as a function of time in Figure 5 for the χ_{00}, χ_{++}, and χ_{+-} models. We note that it takes time for the outflow to develop and propagate out the EM luminosity extraction radius of $150M$, which is why although the flow around the black holes can relax, it takes longer for the EM luminosity to relax. The evolution of the χ_{--} model was long enough for the accretion rate to relax, but not long enough for the EM luminosity to do so. As a result we do not include this model here. The figure clearly demonstrates that spin plays a
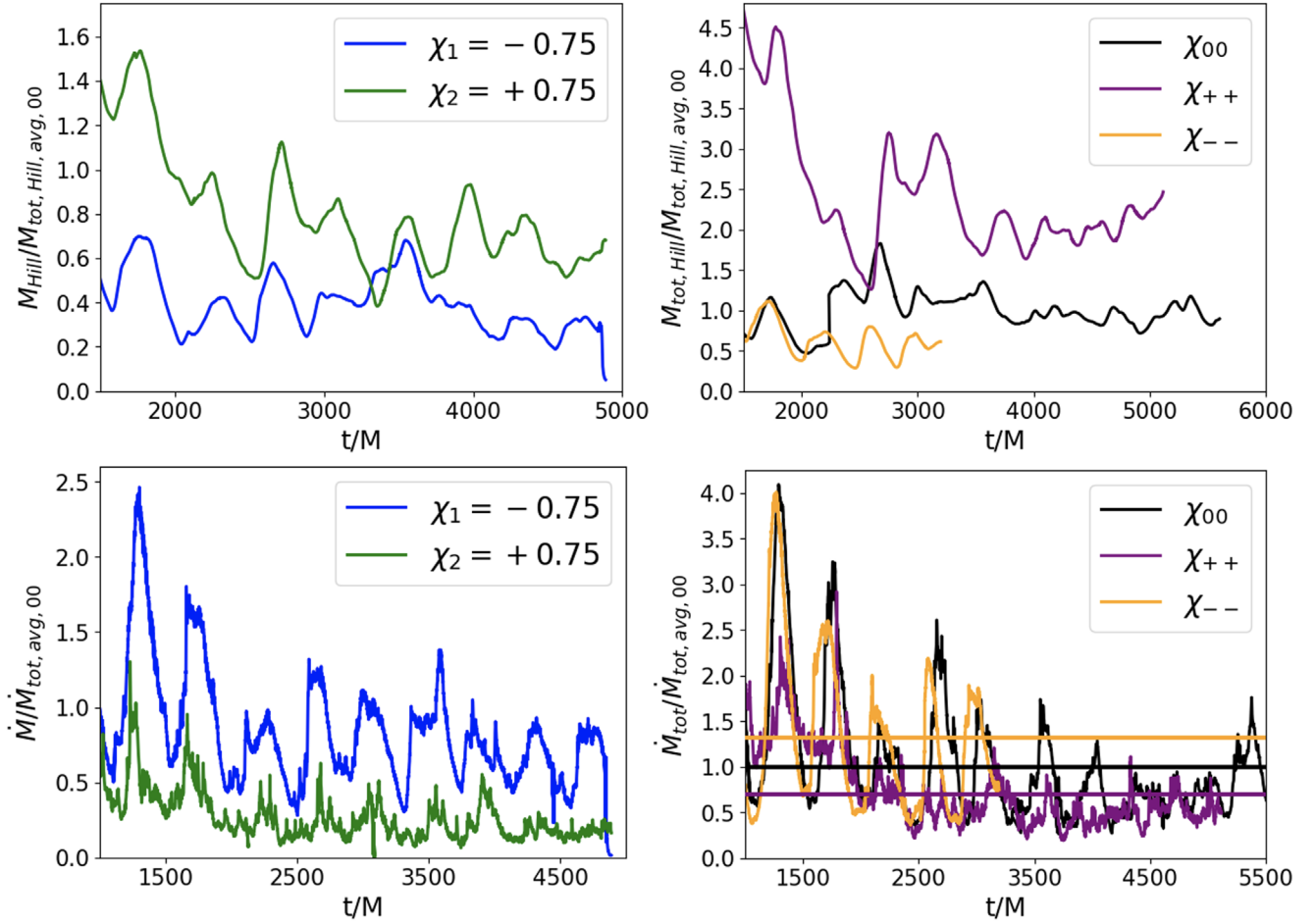
Figure 3. Top left: rest mass within the Hill sphere of each black hole in the χ_{+-} model as a function of time, normalized to the average value for the total rest mass in both Hill spheres for the χ_{00} case. Top right: total rest mass within the Hill spheres of both black holes in each model listed as a function of time, with the same normalization as in the top left. Bottom left: rest-mass accretion rate onto each black hole for the χ_{+-} model as a function of time, normalized to the time-averaged value of the total rest-mass accretion rate onto both black holes in the χ_{00} case. Bottom right: total rest-mass accretion rate onto both black holes in each model listed as a function of time with the same normalization as in the bottom left. The horizontal lines indicate the time-averaged value for each model. $M \approx 5\left(\frac{M}{10^6 M_\odot}\right)$ s.

significant role in the efficiency of the luminosity output, with the greatest efficiency achieved in the χ_{++} model and the lowest efficiency in the χ_{00} model. This is the expected outcome resulting from the combination of the Blandford–Znajek (BZ) effect, which describes outgoing luminosity produced from a single spinning black hole (Blandford & Znajek 1977; see also McKinney & Gammie 2004; Hawley & Krolik 2006 for GRMHD studies on the spin dependence of jet luminosities) and an orbital BZ effect (Palenzuela et al. 2010).

Finally, we compute the effective disk temperature based on the assumption of radiation pressure dominance (consistent with the $\Gamma = 4/3$ equation of state), by solving $\rho_0 \epsilon = a T^4$. We scale the total binary mass to $10^6 M_\odot$ and scale the maximum rest-mass density such that the average accretion rate equals the Eddington accretion rate with efficiency 10%. Doing this provides a characteristic temperature in the minidisks of around $T \sim 10^6 \left(\frac{\dot{M}_{avg}}{\dot{M}_{Edd}}\right)^{1/4} \left(\frac{M}{10^6 M_\odot}\right)^{-1/4}$ K. We find this to be consistent across each of the models. The minidisks have a higher temperature than the circumbinary disk, which is itself hottest at the inner edges and cooler in the bulk of the disk.

4. Conclusions and Discussion

We have demonstrated that minidisks in binary black holes form if the Hill sphere or equivalently the tidal truncation radius is significantly larger than the ISCO radius. We further showed that the size of the minidisks (on average) traces the approximate Hill sphere around each black hole, which implies that the sizes of minidisks are tidally truncated and therefore a simple, linear function of the binary separation only. This finding could be important if the size of minidisks could be inferred from observations. One of the challenges involved is that source size depends on observation frequency, but one may hope that correlations between the actual minidisk size and its photosphere can be found in the future.

Our work establishes a common evolutionary sequence that similar systems are expected to follow: At large enough separations when the Hill sphere is larger than the ISCO radius, minidisks are expected to be present. In this phase the accretion rate could be quasi-periodic with the size of the minidisks depending linearly on the binary separation. Ultimately GRMHD simulations in full GR at large separations are necessary to confirm these expectations and the presence of accretion periodicities on the binary orbital time. Since $r_{\rm Hill} = 0.5(q/3)^{1/3} d$ depends on the binary separation, as the
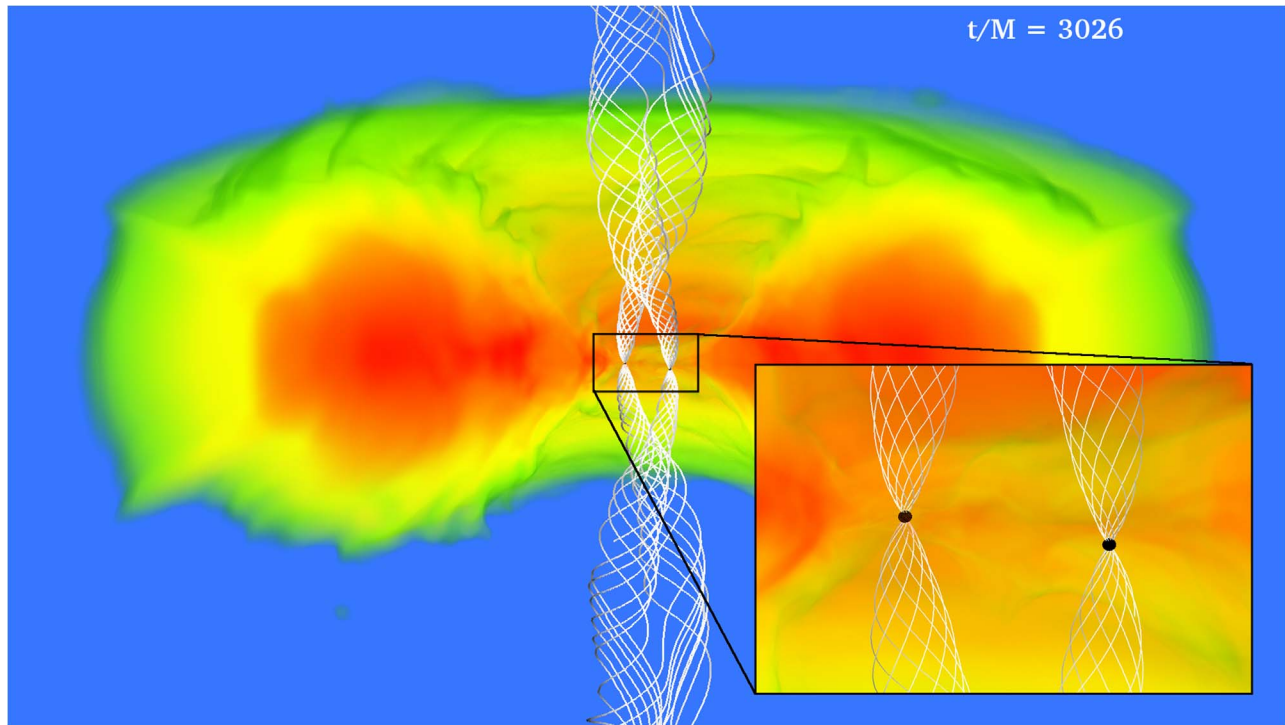
Figure 4. 3D view showing rest-mass density (color coded) for the χ_{++} model and magnetic field lines (white) anchored on the black hole horizons. Twin jets are visible above and below each black hole (see inset for a zoomed-in view). The black spheres indicate the resolved black hole apparent horizons in our simulations.
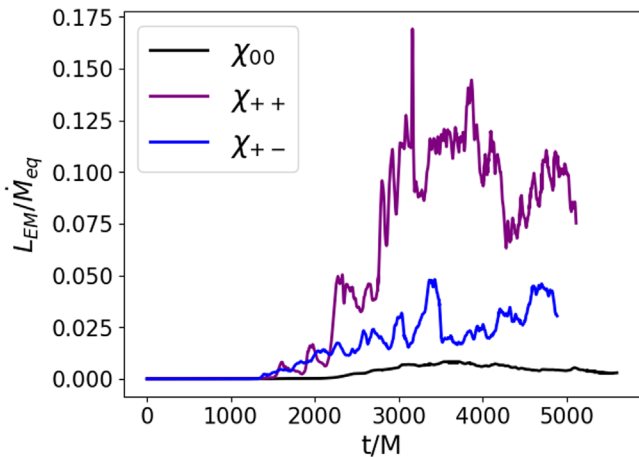

Figure 5. The efficiency for converting accretion power to EM luminosity $L_{EM}/\dot{M}_{eq}$ as a function of time. Here L_{EM} is the Poynting luminosity and $\dot{M}_{eq}$ is the average total rest-mass accretion rate for each model after $t = 1500M$ when the accretion rate has settled, and $M \approx 5 \left(\frac{M}{10^6 M_\odot} \right)$ s.

binary inspirals it will reach a threshold where $r_{\rm Hill} \simeq r_{\rm ISCO}$ and persistent minidisks will no longer be able to exist and will "evaporate" because the tidally stripped accretion streams from the circumbinary disk are accreted on a short dynamical timescale as they plunge into the black hole following ISCO crossing. This leads to more complicated variability in the mass accretion rate until merger and any EM signature associated with persistent minidisks is expected to become fainter. Note that the onset of this transition depends on black hole spin (through the ISCO radius). We term this anticipated dimming of EM emission from minidisks "minidisk evaporation" and expect it to be an inevitable outcome, that is qualitatively robust even for different magnetic field strengths, topologies or initial torus parameters (quantitative measures such as minidisk accretion rates may well depend on the details). Following minidisk evaporation toward the late stages of the inspiral, the qualitative evolution then proceeds in accord with our previously obtained results (Farris et al. 2012; Gold et al. 2014a, 2014b; Khan et al. 2018). Our simulations also suggest that black hole binaries with prograde spin maintain minidisks for a longer timescale than nonspinning and retrograde spin black holes.

These findings could in principle serve as a new diagnostic to probe black hole spins observationally when combined with information from the gravitational wave signal. In particular, when LISA is operating or in the event that Pulsar Timing Arrays detect an individual supermassive black hole binary, the merger time can be predicted from the gravitational wave signal. Therefore, the difference of merger time to the time when the minidisk signature fades away should open a new avenue to probe black hole spins observationally. For this strategy to work out additional source modeling and better predictions from theory will be invaluable. Our work here has shown that when $r_{\rm Hill} \gg r_{\rm ISCO}$, minidisks can form, but additional studies to probe the epoch of minidisk evaporation where $r_{\rm Hill} \gtrsim r_{\rm ISCO}$ will be important to make this a viable and useful diagnostic.

In addition to the minidisk dynamics here we also found that jets arising from circumbinary accretion onto binary black holes toward the late stages of the inspiral are significantly more powerful when spinning black holes (even with moderately high dimensionless spin of $\chi = 0.75$) are involved. With proper theoretical modeling this finding also paves a new way to probe black hole spin from future EM jet observations of these systems.

Finally, apart from the observational implications, our results have important consequences for future relativistic simulations

of these systems. In particular, the chosen initial orbital separation should respect the criterion for minidisk formation in order to properly compute accretion rates and electromagnetic signals, and to faithfully represent the expected structure of the circumbinary system.

ORCID iDs

Vasileios Paschalidis ⬤ https://orcid.org/0000-0002-8099-9023
Milton Ruiz ⬤ https://orcid.org/0000-0002-7532-4144
Roman Gold ⬤ https://orcid.org/0000-0003-2492-1966

References

Amaro-Seoane, P., Audley, H., Babak, S., et al. 2017, arXiv:1702.00786
Ansorg, M., Bruegmann, B., & Tichy, W. 2004, PhRvD, 70, 064011
Armengol, F. G. L., Combi, L., Campanelli, M., et al. 2021, arXiv:2102.00243
Baumgarte, T. W., & Shapiro, S. L. 1999, PhRvD, 59, 024007
Blandford, R. D., & Znajek, R. L. 1977, MNRAS, 179, 433
Bowen, D. B., Campanelli, M., Krolik, J. H., Mewes, V., & Noble, S. C. 2017, ApJ, 838, 42
Bowen, D. B., Mewes, V., Campanelli, M., et al. 2018, ApJL, 853, L17
Bowen, D. B., Mewes, V., Noble, S. C., et al. 2019, ApJ, 879, 76
Charisi, M., Bartos, I., Haiman, Z., et al. 2016, MNRAS, 463, 2145
d'Ascoli, S., Noble, S. C., Bowen, D. B., et al. 2018, ApJ, 865, 140
Drake, A. J., Djorgovski, S. G., Mahabal, A., et al. 2009, ApJ, 696, 870
Farris, B. D., Duffell, P., MacFadyen, A. I., & Haiman, Z. 2014, ApJ, 783, 134
Farris, B. D., Duffell, P., MacFadyen, A. I., & Haiman, Z. 2015, MNRAS, 447, L80
Farris, B. D., Gold, R., Paschalidis, V., Etienne, Z. B., & Shapiro, S. L. 2012, PhRvL, 109, 221102
Farris, B. D., Liu, Y. T., & Shapiro, S. L. 2010, PhRvD, 81, 084008
Giacomazzo, B., Baker, J. G., Miller, M. C., Reynolds, C. S., & van Meter, J. R. 2012, ApJL, 752, L15
Gold, R. 2019, Galax, 7, 63
Gold, R., Paschalidis, V., Etienne, Z. B., Shapiro, S. L., & Pfeiffer, H. P. 2014a, PhRvD, 89, 064060
Gold, R., Paschalidis, V., Ruiz, M., et al. 2014b, PhRvD, 90, 104030
Graham, M. J., Djorgovski, S. G., Stern, D., et al. 2015, MNRAS, 453, 1562
Hawley, J. F., & Krolik, J. H. 2006, ApJ, 641, 103
Hobbs, G., Archibald, A., Arzoumanian, Z., et al. 2010, CQGra, 27, 084013
Hu, B. X., D'Orazio, D. J., Haiman, Z., et al. 2020, MNRAS, 495, 4061
Kelly, B. J., Baker, J. G., Etienne, Z. B., Giacomazzo, B., & Schnittman, J. 2017, PhRvD, 96, 123003
Khan, A., Paschalidis, V., Ruiz, M., & Shapiro, S. L. 2018, PhRvD, 97, 044036
Lynden-Bell, D. 1969, Natur, 223, 690
McKinney, J. C., & Gammie, C. F. 2004, ApJ, 611, 977
Nguyen, K., Bogdanović, T., Runnoe, J. C., et al. 2019, ApJ, 870, 16
Noble, S. C., Mundim, B. C., Nakano, H., et al. 2012, ApJ, 755, 51
Palenzuela, C., Lehner, L., & Liebling, S. L. 2010, Sci, 329, 927
Porth, O., Chatterjee, K., Narayan, R., et al. 2019, ApJS, 243, 26
Reynolds, C. S. 2019, NatAs, 3, 41
Rodriguez, C., Taylor, G. B., Zavala, R. T., Pihlström, Y. M., & Peck, A. B. 2009, ApJ, 697, 37
Roedig, C., Krolik, J. H., & Miller, M. C. 2014, ApJ, 785, 115
Sesana, A., Roedig, C., Reynolds, M., & Dotti, M. 2012, MNRAS, 420, 860
Shibata, M., & Nakamura, T. 1995, PhRvD, 52, 5428